

Synthesis and physicochemical study of Ni^{II} complexes with tetradentate acyclic and macrocyclic N₂S₂ ligands as thiosalen analogs

K. P. Butin,^{a*} A. A. Moiseeva,^a E. K. Beloglazkina,^a Yu. B. Chudinov,^a A. A. Chizhevskii,^a A. V. Mironov,^a B. N. Tarasevich,^a A. V. Lalov,^b and N. V. Zyk^a

^aDepartment of Chemistry, M. V. Lomonosov Moscow State University, 1 Leninskie Gory, 119992 Moscow, Russian Federation.

Fax: +7 (095) 939 5546. E-mail: butin@org.chem.msu.ru

^bN. D. Zelinsky Institute of Organic Chemistry, Russian Academy of Sciences, 47 Leninsky prosp., 119991 Moscow, Russian Federation

N,N'-Polymethylenebis(thiosalicylidene)iminate and macrocyclic dithiadiazadibenzocycloalkadiene complexes of nickel(II) were synthesized and their electrochemical and spectroscopic properties were studied. Dithiadiazadibenzocycloalkadiene complexes containing two DMSO molecules coordinated to Ni²⁺ and two outer-sphere ClO₄⁻ anions were synthesized by the reaction of the corresponding macrocyclic ligands with Ni(ClO₄)₂·6H₂O. The structure of 3,6-dithia-10,14-diazadibenzo[*a,g*]cyclopentadeca-9,14-dienylnickel(II)[bis(dimethyl sulfoxide) bis-perchlorate] was established by X-ray diffraction. The UV-Vis spectroscopic data are consistent with octahedral structures of diiminobis(sulfide) complexes, a square-planar structure of the thiosalen complex, and distorted tetrahedral structures of other diiminodithiolate complexes. The reaction of *S-tert*-butylthiosalicylaldehyde with hydrazine hydrate afforded di(*ortho-tert*-butylthiobenzal)azine. The reaction of the latter with anhydrous NiCl₂ produced a colored complex with the simplest molecular formula Ni(C₁₆H₁₂N₂S₂) in 15% yield. Semiempirical PM3(tm) calculations and the results of UV-Vis, ESR, and ¹H NMR spectroscopy demonstrate that this complex has most probably a dimeric structure, in which two Ni centers adopt a nearly square-planar configuration. The complexes are clearly divided into two types according to their electrochemical behavior in DMF solutions. The type 1 is characterized by reversibility of the first reduction steps. The type 2 is characterized by irreversible two-electron reduction as the first step accompanied by deposition of Ni metal on the electrode surface. Rapid electrochemically initiated alkylation occurs in the presence of various alkylating agents (BuⁿI, BuⁿBr, (DmgH)₂CoCH₃) in a solution of complex **1** in DMF.

Key words: nickel(II), thiosalen, homoleptic thiosalen complexes, diiminobis(sulfide) complexes, macrocyclic *S,S*-alkylidenethiosalicylimines, electrochemistry, UV-Vis spectroscopy, 3,6-dithia-10,14-diazadibenzo[*a,g*]cyclopentadeca-9,14-dienylnickel(II) bis-dimethyl sulfoxide bis-perchlorate, crystal and molecular structures.

Transition metal complexes with the tetradentate N₂X₂ ligands, which are Schiff bases, *viz.*, alkylenediamine derivatives (N is imine nitrogen; X = O⁻ (salen), S⁻ (thiosalen), OR, SR, PR₂, *etc.*), have catalytic activity in many reactions. Salen (*N,N'*-ethylenebis(salicylideneiminate)) and its derivatives are the most well known tetradentate Schiff bases, which form rigid planar coordination about the central metal ion.¹ Achiral and chiral salen complexes of middle and late transition metals catalyze alkene epoxidation, including asymmetric epoxidation,^{2–4} cyclopropanation,⁵ aziridination,⁶ sulfide oxidation,^{7,8} the Diels–Alder reaction,⁹ activation of C–H bonds,^{10–12} and asymmetric epoxide ring opening.^{13–18}

Salen complexes of Co^{II} and Ni^{II} are extensively studied as potential catalysts for electrochemical reduction of organic halides (see, for example, the study¹⁹ and references cited therein). In recent years, electrochemical activation of freons has attracted attention in connection not only with problems of ozone layer destruction but also with a search for ways of converting facilities from freon production to new freon alternative products.²⁰ Recently,²¹ Ni^{II}(Salen) has been proposed as an efficient electrocatalyst for reduction of polyfluoroalkyl chlorides.²¹

Salen complexes are used also as model compounds to elucidate the mechanisms of action of particular enzymes. For example, the Mn^{III}(Salen) complex simulates the action of Mn-containing forms of superoxide dismutase,²²

and the Fe^{III}(Salen) complex simulates the action of enzymes responsible for sulfoxidation of organic sulfides.²³

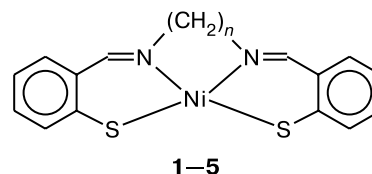
In the present study, we synthesized Ni^{II} complexes with tetradentate acyclic and macrocyclic N₂S₂ ligands (thiosalen analogs) and investigated them by electrochemical methods. Sulfur-containing ligands have attracted our attention due primarily to the fact that metal atoms in natural metalloenzymes are often coordinated by the sulfur atom of cysteine or methionine. However, there is no simple and unambiguous answer to the question of why metal atoms in some natural enzymes are bound to sulfur, whereas metal atoms in other enzymes are bound to oxygen. The present study was aimed at synthesizing Ni^{II} complexes with different coordination modes and geometry and examining the effect of the electronic structure and geometry of the ligand on the redox potential and reactivity of the reduced forms of the complexes (with metals in low oxidation states, *viz.*, Ni^I and Ni⁰) in alkylation at the metal atoms.

Complexes of thiosalen and its homologs and analogs with metals have been studied in much less detail compared to salen complexes (see, for example, the studies^{24,25} and references cited therein). The replacement of two phenoxide oxygen atoms in salen by two thiolate sulfur atoms giving rise to thiosalen should, in principle, lead to changes in the redox properties of the corresponding complexes. Since sulfur is a medium-strength soft base, whereas oxygen is a strong hard base, it is often expected (see the studies^{26,27} and references cited therein) that coordination by sulfur will stabilize metal in low oxidation states (for example, Ni^I), *i.e.*, lead to a decrease in the potential of the Ni^{II}/Ni^I transition. However, even attempts to explain the known facts in terms of the simple principle of hard and soft acids and bases are complicated by the fact that nickel can be considered as either hard or soft depending not only on its oxidation state but also on the nature of the ligands.²⁶

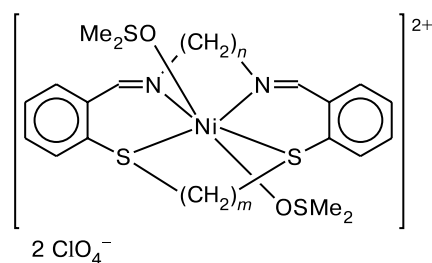
Results and Discussion

Synthesis of Ni^{II} thiosalicylimine complexes

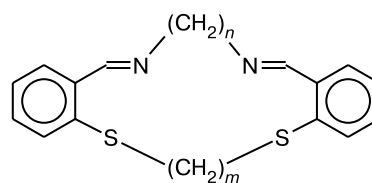
We studied Ni^{II} thiosalicylimine complexes. Compounds **1–5** are complexes with charged iminothiolate-



1–5

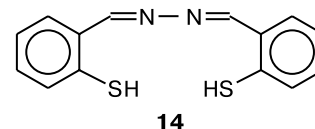


6–9



10–13

	1	2	3	4	5	6, 10	7, 11	8, 12	9, 13
<i>n</i>	2	3	4	6	8	2	2	3	3
<i>m</i>	—	—	—	—	—	2	3	2	3

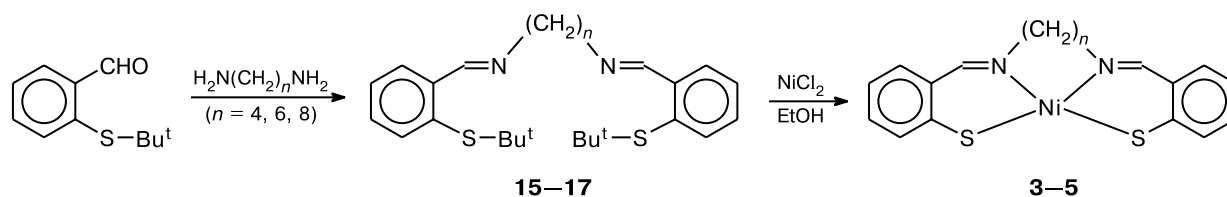


14

type ligands. Compounds **6–9** are complexes with uncharged diiminobis(sulfide) ligands and, hence, they contain counterions (perchlorate ions). The structure of nickel di(*ortho*-thiobenzal)azine complex **14** is discussed below.

Complexes **1** (nickel thiosalen complex)²⁸ and **2**²⁹ were synthesized according to procedures developed earlier. The previously unknown nickel diiminodithiolate complexes containing more than three methylene groups between the amino groups were prepared according to a

Scheme 1



Compound	3	4	5	15	16	17
<i>n</i>	4	6	8	4	6	8
Yield (%)	72	60	35	99	99	99

Table 1. Spectroscopic data and results of elemental analysis for ligands and intermediate products of their synthesis

Compound	Found / Calculated (%)			¹ H NMR (CDCl ₃) δ*	IR /cm ⁻¹
	C	H	N		
3,6-Dithia-10,13-diazadibenzo[<i>a,g</i>]-cyclohexadeca-9,13-diene (10)	<u>65.91</u> 66.22	<u>5.67</u> 5.56	<u>9.02</u> 8.58	2.83 (s, 4 H, CH ₂ S); 3.97 (s, 4 H, CH ₂ N); 7.20 (t, 2 H, H _{arom}); 7.43 (d, 2 H, H _{arom}); 7.74 (d, 2 H, H _{arom}); 8.80 (s, 2 H, HC=N)	1690
3,7-Dithia-11,14-diazadibenzo[<i>a,h</i>]-cyclopentadeca-10,14-diene (11)	<u>66.85</u> 67.02	<u>5.70</u> 5.92	<u>8.46</u> 8.23	1.84 (m, 2 H, CH ₂); 2.83 (t, 4 H, CH ₂ S); 3.70 (t, 4 H, CH ₂ N); 7.29 (t, 2 H, H _{arom}); 7.39 (t, 2 H, H _{arom}); 7.50 (d, 2 H, H _{arom}); 7.68 (d, 2 H, H _{arom}); 8.64 (s, 2 H, HC=N)	1695
3,6-Dithia-10,14-diazadibenzo[<i>a,g</i>]-cyclopentadeca-9,14-diene (12)	<u>67.05</u> 67.02	<u>5.97</u> 5.92	<u>8.46</u> 8.23	1.85–1.90 (t, 2 H, CH ₂); 2.95 (s, 4 H, CH ₂ S); 3.82 (t, 4 H, CH ₂ N); 7.22 (t, 2 H, H _{arom}); 7.41 (t, 2 H, H _{arom}); 7.80 (d, 2 H, H _{arom}); 7.81 (d, 2 H, H _{arom}); 8.80 (s, 2 H, HC=N)	1695
3,7-Dithia-11,15-diazadibenzo[<i>a,h</i>]-cyclohexa-10,15-diene (13)	<u>66.98</u> 67.76	<u>6.24</u> 6.25	<u>8.41</u> 7.90	2.08 (m, 2 H, CH ₂); 2.95 (m+t, 2 H, CH ₂ +4 H, CH ₂ S); 3.68 (t, 4 H, CH ₂ N); 7.22 (m, 2 H, H _{arom}); 7.30 (t, 2 H, H _{arom}); 7.95 (d, 2 H, H _{arom}); 8.80 (s, 2 H, HC=N)	1700
<i>N,N'</i> -Tetramethylenebis(<i>ortho-tert</i> -butylthiobenzal)diimine (15)	<u>70.78</u> 70.86	<u>7.95</u> 8.23	<u>7.91</u> 6.36	1.06 (s, 18 H, Bu ^t); 1.74 (m, 4 H, CH ₂); 3.65 (m, 4 H, CH ₂ N); 7.22 (m, 2 H, H _{arom}); 7.42, 7.54 (both t, 2 H each, H _{arom}); 7.51, 7.87 (both d, 2 H each, H _{arom}); 7.96, 8.01 (both d, 2 H each, H _{arom}); 8.62, 9.01 (both s, 2 H each, 1 : 1, HC=N)	1700
<i>N,N'</i> -Hexamethylenebis(<i>ortho-tert</i> -butylthiobenzal)diimine (16)	<u>71.49</u> 71.74	<u>8.80</u> 8.60	—	1.04 (s, 18 H, Bu ^t); 0.90–1.86 (m, 8 H, CH ₂); 3.70 (m, 4 H, CH ₂ N); 7.15 (m, 2 H, H _{arom}); 7.08, 7.27 (both t, 2 H each, H _{arom}); 7.44, 7.68 (both d, 2 H each, H _{arom}); 7.82, 8.02 (both d, 2 H each, H _{arom}); 8.78, 8.89 (both s, 2 H each, 1 : 1, HC=N)	1700
<i>N,N'</i> -Octamethylenebis(<i>ortho-tert</i> -butylthiobenzal)diimine (17)	<u>72.48</u> 72.53	<u>8.88</u> 8.93	—	—	1700
Di(<i>ortho-tert</i> -butylthiobenzal)-azine (20)	<u>68.12</u> 68.75	<u>7.22</u> 7.29	<u>7.33</u> 7.29	—	1700

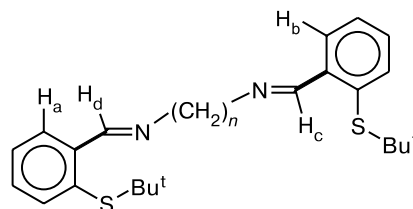
* All spin-spin coupling constants of the aromatic fragments and CH₂ groups are 8.7–8.8 and 6.6–6.8 Hz, respectively.

procedure, which has been used earlier³⁰ to synthesize nickel thiosalen complex **1**. This procedure involves the preparation of di(*ortho-tert*-butylthiobenzal)diimine followed by its reaction with nickel chloride, which is accompanied by thioether bond cleavage to form a metal thiolate complex (Scheme 1).

Diimines **15–17** were identified by IR and ¹H NMR spectroscopy and their compositions were confirmed by elemental analysis (Table 1).

It should be noted that the ¹H NMR spectra of compounds **15–17** show two signals of the HC=N group (in a ratio of 1 : 1) and two sets of signals for aromatic protons. This may be evidence that the bulky *tert*-butyl group hinders free rotation about the C_{arom}–C(=N) bond, so that the H_a–H_b and H_c–H_d protons become nonequivalent and have different chemical shifts (see Table 1).

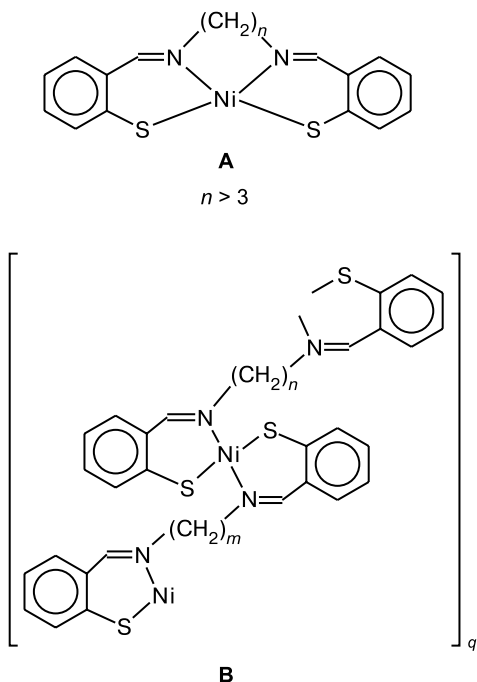
Complexes **3–5** are poorly soluble in all solvents used in the present study. In the IR spectra of these complexes,



the stretching band of the imino group is shifted to longer wavelengths (1635–1625 cm⁻¹) compared to that of the starting ligand (to 1700 cm⁻¹).

Ligands **15–17** can form complexes of two structural types and can be coordinated as either tetradentate ligands (**A**) (resulting complexes have a nickel-containing ring of size *n*+3) or bis-bidentate ligands (**B**) (polymeric complexes).

In the subsequent discussion, we arbitrarily assign the structure **A** to the complexes synthesized. However, an



unambiguous choice between the structures **A** and **B** can be made only based on the results of X-ray diffraction study.

We prepared diiminobis(sulfide) complexes **6–9** for the first time by the reactions of the corresponding macrocyclic ligands **10–13** with nickel perchlorate. Earlier,²⁵ Ni^{II} complexes with neutral ligands of the di(*S*-alkylthio-salicyl)diimine series containing iodide, bromide, or per-

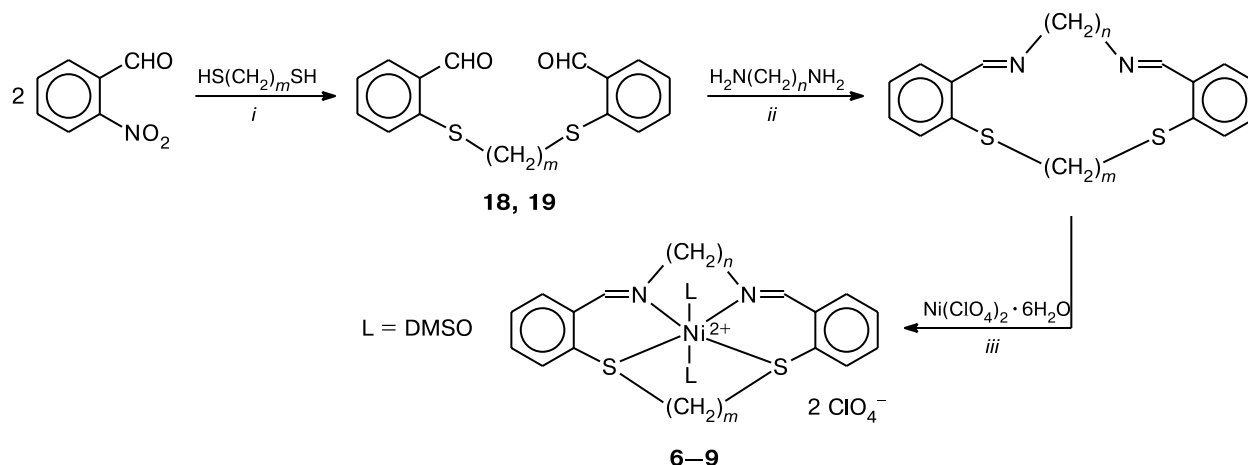
chlorate anions as counterions have been synthesized. However, examples of complexation of Ni^{II} with macrocyclic *S,S*-dialkylthiosalicylimine ligands, which contain polymethylene bridges between both the nitrogen and sulfur atoms,* are lacking in the literature. The macrocyclic ligands and their complexes with nickel(II) were synthesized according to Scheme 2.

In the first step of the synthesis, bis(*ortho*-formylphenyl)-1,4-dithiabutane (**18**) and bis(*ortho*-formylphenyl)-1,5-dithiapentane (**19**) were prepared by nucleophilic displacement of the nitro group in *ortho*-nitrobenzaldehyde with 1,2-ethanedithiol or 1,3-propanedithiol in DMF in the presence of K₂CO₃. Then diformylbis(sulfides) **18** and **19** were used in the reactions with 1,2-diaminobutane or 1,3-diaminopropane. The reactions were carried out in MeOH or EtOH at room temperature, and anhydrous MgSO₄ was added to bind water that was eliminated. The reactions produced the corresponding macrocyclic diiminobis(sulfides) (**10–13**). In the final step of the synthesis, macrocyclic ligands (**10–13**) were used for complexation with Ni(ClO₄)₂·6H₂O to prepare complexes **6–9** containing two DMSO molecules (elemental analysis data).

We also examined the possibility of preparing nickel di(*ortho*-thiobenzal)azine complex **14** containing a single bond between two nitrogen atoms, which is an analog of

* Only the Cu^{II} complex with the thio-salen-type macrocyclic diiminobis(sulfido) ligand, in which two S atoms are linked by the $-(CH_2)_2-$ bridge and two N atoms are linked by the *o,o'*-biphenylene bridge, has been described in the literature.³⁰

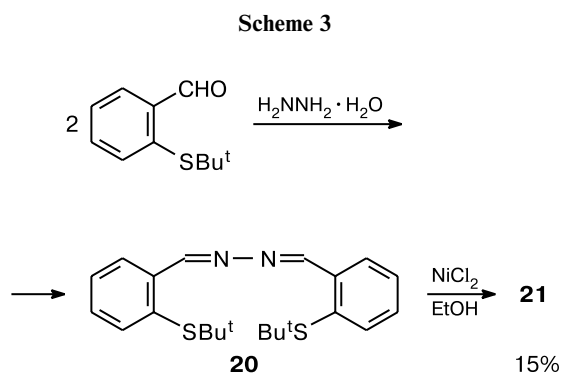
Scheme 2



Compound	6	7	8	9	18	19
Yield (%)	13	30	57	36	38	56
<i>n</i>	2	2	3	3	—	—
<i>m</i>	2	3	2	3	2	3

i. K₂CO₃, DMF. *ii.* EtOH or MeOH, MgSO₄ anhydrous. *iii.* EtOH/CH₃CN/DMSO.

diiminodithiolate complexes **1**–**5**. The synthesis was carried out using a sequence of reactions analogous to that employed for the preparation of complexes **3**–**5**. In the first step, the reaction of hydrazine with *tert*-butylthiosalicylaldehyde afforded azine **20**, which was then used in the reaction with anhydrous NiCl_2 (Scheme 3).



Elemental analysis demonstrated that the composition of complex **21** corresponds to the simplest molecular formula $\text{Ni}(\text{C}_{16}\text{H}_{12}\text{N}_2\text{S}_2)$. The fact that the complex contains the metal ion coordinated by the nitrogen atom is also confirmed by IR spectroscopy (vibrational band of the C=N group, which is observed at 1700 cm^{-1} in the spectrum of di(*ortho-tert*-butylthiobenzal)azine **20**, is shifted to 1615 cm^{-1} in the spectrum of complex **21**; see Tables 1 and 2).

Crystal and molecular structure of complex **8**

The structure of complex **8** was established by X-ray diffraction. Earlier,³¹ a square-planar coordination of metal atoms has been revealed for uncharged dithiolate-type thiosalen complexes of divalent metals, including nickel complex **1**. A square-planar configuration was found also in compounds (analogous to *N,N*-trimethylene-bridged complex **2**) containing substituents in the benzene rings.²⁴ However, the planes of the benzene rings in these compounds deviate from the S_2N_2 plane by $\sim 35^\circ$. In the bis-sulfide-type anionic Ni^{II} bis(hexylthio)salen complex, the metal atom has an octahedral coordination involving two Br^- ions as axial ligands.²⁵ The Ni–N and Ni–S bonds in this complex are longer than those in planar complex **1**, *i.e.*, the Ni atom in the high-spin complex forms a weaker bond with N_2S_2 compared to the corresponding bond in low-spin complex **1**. An elongation of the Ni–ligand bonds may be attributable either to the fact that the $d_{x^2-y^2}$ orbital in the octahedral complex, unlike that in the square-planar complex, is occupied or to distortion of the ligand geometry in the former complex.

The crystallographic data, characteristics of X-ray diffraction study, and results of structure refinement of com-

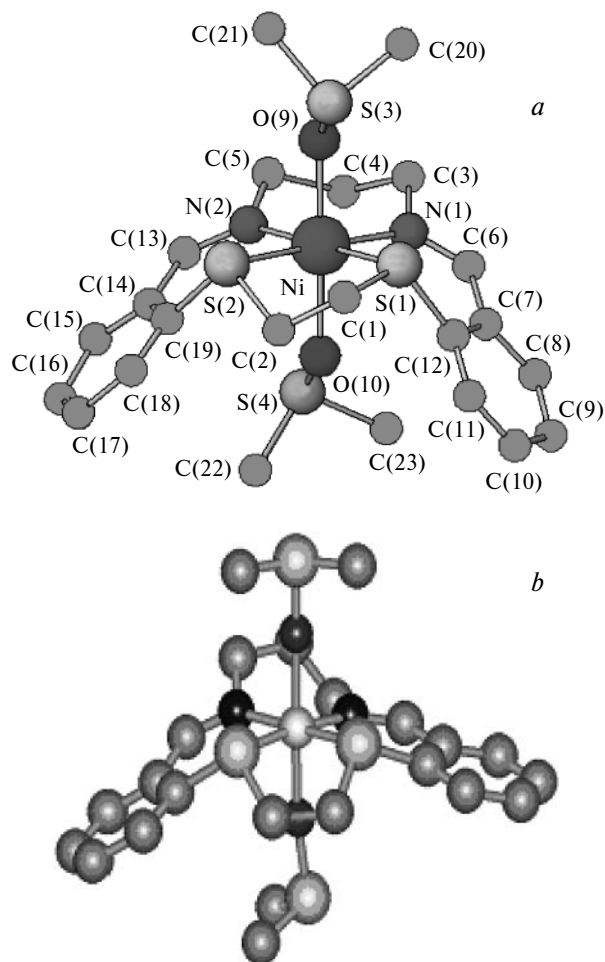


Fig. 1. Crystallographic molecular structure of the $[\mathbf{12} \cdot \text{Ni}(\text{DMSO})_2]^{2+}$ dication (*a*) and the structure calculated by the PM3(tm) method (*b*).

pound **8** are given in Table 3. Selected bond lengths and bond angle are listed in Table 4. The structure of the $[\mathbf{12} \cdot \text{Ni}(\text{DMSO})_2]^{2+}$ dication (**8**) is shown in Fig. 1. The central nickel atom has an octahedral coordination with two DMSO molecules as axial ligands. The Ni atom lies almost strictly in a plane passing through the N_2S_2 atoms of the macrocyclic ligand (deviation is $0.050(13)\text{ \AA}$). Analysis of the data on the octahedral Ni^{II} complexes retrieved from the Cambridge Structural Database³² demonstrated that the Ni–N ($2.031(12)$ and $2.027(11)\text{ \AA}$) and Ni–S ($2.398(4)$ and $2.381(4)\text{ \AA}$) distances vary in ranges typical of Ni–NC (2.006 – 2.212 \AA , 41 records) and Ni–S(Alkyl)Ar (2.344 – 2.575 \AA , 48 records) bonds, respectively. The S–Ni–N, S–Ni–O, and N–Ni–O angles are close to 90° . The S(1)–Ni–S(2) angle is slightly smaller than 90° , whereas the N(1)–Ni–N(2) angle is, on the contrary, slightly larger than 90° , which is, apparently, associated with the difference in the number of carbon atoms in the bridges between the N atoms and the S atoms in the chelating rings. The planes of the benzene

Table 2. Physicochemical and spectroscopic data for complexes 3–9

Compound	Crystal color	M.p. /°C	Found / Calculated (%)			¹ H NMR (DMSO-d ₆), ^a δ	IR /cm ⁻¹
			C	H	N		
<i>N,N'</i> -Tetramethylene-bis(thiosalicylideneiminato)-nickel(II) (3)	Pale-green	102–107 (разл.)	<u>56.12</u> 56.13	<u>4.24</u> 4.24	<u>7.19</u> 7.27	Very poorly soluble — ^b	1625
<i>N,N'</i> -Hexamethylene-bis(thiosalicylideneiminato)-nickel(II) (4)	Pale-green	78–83 (разл.)	<u>57.67</u> 58.13	<u>4.93</u> 5.37	<u>6.79</u> 6.78	Very poorly soluble — ^b	1630
<i>N,N'</i> -Octamethylene-bis(thiosalicylideneiminato)-nickel(II) (5)	Pale-green	70–74 (разл.)	<u>59.36</u> 59.88	<u>5.34</u> 5.94	<u>6.09</u> 6.35	Very poorly soluble — ^b	1635
3,6-Dithia-10,13-diazadi-benzo[<i>a,g</i>]cyclotetradeca-9,13-dienylnickel(II)[bis(dimethyl sulfoxide) bis-perchlorate] (6)	Red	270 ^c	<u>35.90</u> 35.69	<u>3.74</u> 4.08	<u>3.94</u> 4.08	3.02 (s, 4 H, CH ₂ S); 3.86 (s, 4 H, CH ₂ N); 7.28 (t, 2 H, H _{arom}); 7.46 (d, 2 H, H _{arom}); 7.60 (d, 2 H, H _{arom}); 7.90 (t, 2 H, H _{arom}); 8.80 (s, 2 H, HC=N)	1625
3,7-Dithia-11,14-diazadi-benzo[<i>a,h</i>]cyclopentadeca-10,14-dienylnickel(II)[bis(dimethyl sulfoxide) bis-perchlorate] (7)	Красно-коричневый	165 ^c	<u>36.95</u> 36.62	<u>4.21</u> 4.28	<u>4.28</u> 3.71	—	1630
3,6-Dithia-10,14-diazadi-benzo[<i>a,g</i>]cyclopentadeca-9,14-dienylnickel(II)[bis(dimethyl sulfoxide)bis-perchlorate] (8)	Оливково-зелен	205 ^c	<u>36.95</u> 36.62	<u>3.99</u> 4.28	<u>3.54</u> 3.71	2.15 (m, 2 H, CH ₂); 3.05 (s, 4 H, CH ₂ S); 4.00 (t, 4 H, CH ₂ N); 7.30 (t, 2 H, H _{arom}); 7.38 (d, 2 H, H _{arom}); 7.50 (d, 2 H, H _{arom}); 7.77 (t, 2 H, H _{arom}); 8.69 (s, 2 H, HC=N)	1630
3,7-Dithia-11,15-diazadi-benzo[<i>a,h</i>]cyclohexadeca-10,15-dienylnickel(II)[bis(dimethyl sulfoxide)bis-perchlorate] (9)	Оливково-зелен	162 ^c	<u>36.89</u> 37.52	<u>3.66</u> 3.65	<u>4.81</u> 4.46	2.20 (m, 2 H, CH ₂); 2.90 (m+t, 2 H, CH ₂ +4 H, CH ₂ S); 3.78 (t, 4 H, CH ₂ N); 7.25 (m, 4 H, H _{arom}); 7.42 (t, 2 H, H _{arom}); 7.93 (t, 2 H, H _{arom}); 8.70 (s, 2 H, HC=N)	1635
Ni(C ₁₆ H ₁₂ N ₂ S ₂) ^d (21)	Body color	130–135 ^c (разл.)	<u>51.42</u> 51.10	<u>3.00</u> 3.06	<u>8.53</u> 8.51	7.90 (t, 2 H, H _{arom}); 7.98 (t, 2 H, H _{arom}); 8.32 (d, 2 H, H _{arom}); 8.24 (d, 4 H, H _{arom}); 9.12 (s, 2 H, HC=N)	1615

^a All spin-spin coupling constants of the aromatic fragments and CH₂ groups are 8.7–8.8 and 6.6–6.8 Hz, respectively.

^b In DMF-d₇.

^c For perchlorates, the decomposition temperatures are given (without premelting).

^d The mass spectrum (direct probe, electron impact, 70 eV), *m/z* (*I* (%)): 299 (25%, M-29, M – N₂H, or M – CH₂NH), 135 (75%, C₆H₄CHNS), 103 (20%, C₆H₅CN), 91 (85%, C₇H₇), 77 (100%, C₆H₅), 64 (40%, C₅H₄), 51 (50%, C₄H₃). The fragments with peak intensities of no lower than 20% are given. No peaks at *m/z* > 299 are observed.

rings are inclined to the basal plane of the complex determined by the N, N, S, and S atoms (43.6(5)° and 55.3(4)°) and are located on the same side of this plane, whereas three carbon atoms of the trimethylene group between the nitrogen atoms are located on the opposite side of the basal plane. This configuration is, apparently, associated

with the chair conformation of the six-membered NiN₂C₃ ring, and the difference in the inclination angles of the benzene rings is attributable to nonlinearity of the carbon chain between the sulfur atoms. The distances from the C(1) and C(2) atoms to the nearest atoms of the benzene rings (C(12) and C(19), respectively) are virtually equal

Table 3. Crystallographic data, details of X-ray diffraction study, and characteristics of structure refinement for compound **8**

Molecular formula	C ₂₃ H ₃₂ Cl ₂ N ₂ NiO ₁₀ S ₄
Molecular weight	694.03
Space group	<i>P</i> 2 ₁ / <i>a</i>
Unit cell parameters:	
<i>a</i> /Å	15.600(4)
<i>b</i> /Å	11.985(1)
<i>c</i> /Å	17.302(3)
β/deg	103.72(2)
<i>V</i> /Å ³	3143(2)
Number of formula units	4
Calculated density/g cm ⁻³	1.594
Linear absorption coefficient/cm ⁻¹	11.08
Absorption correction	ψ scanning technique
<i>T</i> _{min} / <i>T</i> _{max}	0.933
<i>F</i> (000)	1560
θ range/deg	2–25
Scanning mode	ω/1.33θ
Ranges of reflection indices	−4 ≤ <i>h</i> ≤ 18, 0 ≤ <i>k</i> ≤ 14, −20 ≤ <i>l</i> ≤ 20
Number of measured reflections	2848
Number of independent reflections	2179
<i>R</i> _{int} = 0.014	
Number of reflections with <i>I</i> > 3σ(<i>I</i>)	2074
Number of refinement variables	379
Least-squares refinement against <i>F</i>	
Goodness-of-fit	1.360
<i>R</i> factors based on reflections with <i>I</i> > 3σ(<i>I</i>)	
<i>R</i>	0.068
<i>wR</i>	0.095
Residual density (e _{max} /e _{min}), e/Å ⁻³	0.53/−0.94

to each other (2.87 Å), whereas the deviations of the C(1) and C(2) atoms from the S₂N₂ plane are substantially different (0.31 and 0.97 Å, respectively).

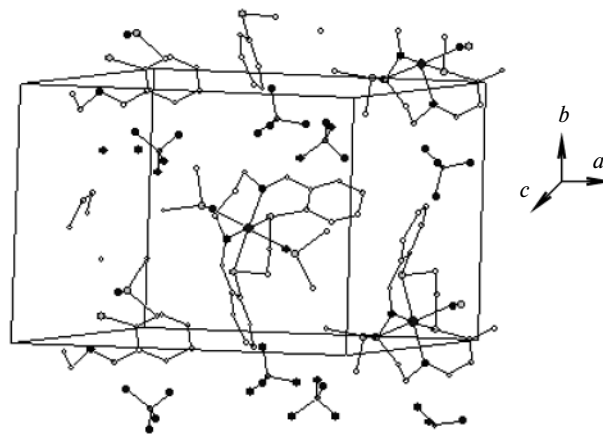
The crystal structure of complex **8** is shown in Fig. 2. The [12 · Ni(DMSO)₂]²⁺ dications form layers parallel to the (010) plane alternating with the layers formed by the ClO₄[−] anions.

The molecular geometry of the [12 · Ni(DMSO)₂]²⁺ dication calculated by the semiempirical PM3(tm) method³⁴ is, in principle, identical to that determined by

X-ray diffraction analysis (see Fig. 1). The planes of the benzene rings are located on the same side of the basal plane of the complex, whereas three carbon atoms of the polymethylene fragment between the nitrogen atoms are located on the opposite side. However, the six-membered NiN₂C₃ ring in the calculated structure, unlike that in the

Table 4. Selected interatomic distances (*d*) and bond angles (ω) for compound **8**

Bond	<i>d</i> /Å	Angle	ω/deg
Ni—N(1)	2.035(10)	N(1)—Ni—N(2)	97.6(4)
Ni—N(2)	2.029(10)	S(1)—Ni(1)—S(2)	85.3(3)
Ni—S(1)	2.394(5)	N(2)—Ni(1)—S(1)	175.0(3)
Ni—S(2)	2.383(4)	N(2)—Ni—S(2)	90.4(3)
Ni—O(9)	2.057(11)	S(1)—Ni—O(10)	90.0(3)
Ni—O(10)	2.130(9)	S(2)—Ni—O(10)	88.6(3)
S(3)—O(9)	1.455(10)	N(1)—Ni—O(10)	91.1(4)
S(4)—O(10)	1.519(9)	N(1)—Ni—O(9)	90.1(4)

**Fig. 2.** Crystal structure of complex **8**.

experimental structure, adopts a twist-boat conformation rather than an ideal chair-like conformation.

Since crystallographic data for complexes **3–5** are lacking, we carried out semiempirical PM3(tm) calculations for a series of complexes analogous to Ni^{II}(Thiosalen), in which the number of the bridging CH₂ groups varied from 1 to 11. The calculations demonstrated that the complexes with $n = 1$ or 2 are planar. However, the improper NSSN dihedral angle gradually increases from 0° to 23° as n increases from 1 to 6 and then remains constant (21–22°) for larger n . Consequently, the coordination of the isolated molecule tends to change from low-spin square-planar to high-spin pseudotetrahedral with increasing n .

UV-Vis spectroscopic study

The spectra of macrocyclic ligand **13** in DMF solutions show a very intense absorption maximum at 316 nm (31645 cm⁻¹) (ϵ 36500 dm³ mol⁻¹ cm⁻¹) associated with intraligand charge transfer. In the spectrum of complex **9** containing ligand **13**, this maximum is slightly hypsochromically shifted to 308 nm (32467 cm⁻¹) and the extinction coefficient sharply decreases to 1895 dm³ mol⁻¹ cm⁻¹ due, presumably, to additional coordination by the solvent (DMF) molecules. Theoretically, three low-intensity (ϵ 1–10 dm³ mol⁻¹ cm⁻¹) spin-allowed d,d transitions, *viz.*, ³A_{2g}→³T_{2g} (at 8000–10000 cm⁻¹), ³A_{2g}→³T_{2g} (13000–15000 cm⁻¹), and ³A_{2g}→³T_{2g} (2400–27000 cm⁻¹), and even less intense spin-forbidden transitions to the ¹D and ¹G states should be observed for octahedral or pseudooctahedral high-spin Ni^{II} complexes.¹ However, we failed to unambiguously reveal absorption bands in these spectral regions because of very poor solubility of the complexes in all solvents. If these bands are present, their intensity is at most 5 dm³ mol⁻¹ cm⁻¹. For complexes **6** and **7**, a charge-transfer band was observed at 311 nm (32154 cm⁻¹, ϵ 3050 dm³ mol⁻¹ cm⁻¹) and 319 nm (31348 cm⁻¹, ϵ 1600 dm³ mol⁻¹ cm⁻¹), respectively. The octahedral Ni(H₂O)₆²⁺(ClO₄⁻)₂ complex is much more readily soluble, and its spectrum in DMF solutions at a concentration of 4·10⁻³ mol L⁻¹ shows pronounced bands at 692 nm (14450 cm⁻¹, ϵ 7.5 dm³ mol⁻¹ cm⁻¹), 618 nm (16181 cm⁻¹, ϵ 6.25 dm³ mol⁻¹ cm⁻¹), and 412 nm (24272 cm⁻¹, ϵ 12.5 dm³ mol⁻¹ cm⁻¹) and a shoulder at 283 nm (35336 cm⁻¹, ϵ 7200 dm³ mol⁻¹ cm⁻¹) corresponding to charge transfer.

The spectrum of thiosalen complex **1** corresponds to that expected for a low-spin square-planar Ni^{II} complex. It has a singlet at 454 nm (22026 cm⁻¹, 1640 dm³ mol⁻¹ cm⁻¹) and the second band at 388 nm (25773 cm⁻¹, ϵ 7200 dm³ mol⁻¹ cm⁻¹). The third, even more intense, band at 295 nm (33898 cm⁻¹,

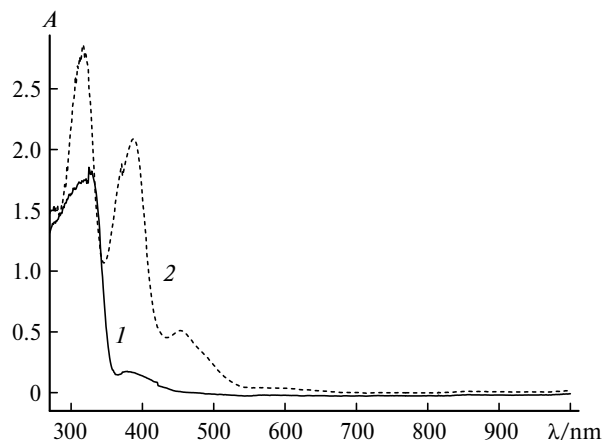


Fig. 3. UV-Vis spectra of complexes **1** (*1*) and **21** (*2*) (DMF, 10⁻³ mol L⁻¹).

ϵ 18600 dm³ mol⁻¹ cm⁻¹) belongs, apparently, to the intraligand transfer (Fig. 3).

In the spectra of complexes **3–5**, no intense bands were found at $\lambda > 256$ nm. In the spectrum of complex **2**, a transition at 304 nm (32894 cm⁻¹) was observed, but this band disappeared within 5 min after dissolution in DMF and the initially brown solution turned almost colorless. In solutions, complexes **3–5** and, probably, complex **2**, unlike complex **1**, have, presumably, pseudotetrahedral or (due to coordination by the solvent) pseudooctahedral or square-pyramidal structures rather than square-planar structures. For a pseudotetrahedral coordination, three bands at 4000–7000 cm⁻¹ (ϵ 10–50 dm³ mol⁻¹ cm⁻¹), 7000–11000 cm⁻¹ (ϵ 100–200 dm³ mol⁻¹ cm⁻¹), and 15000–20000 cm⁻¹ (ϵ 250–500 dm³ mol⁻¹ cm⁻¹)¹ should be observed, whereas bands at wavelengths shorter than 20000 cm⁻¹ should be absent (except for transitions associated with the organic ligand). These compounds should be weakly colored compared to square-planar complexes, and this is actually the case (see Table 2).

Electrochemical study

Electrochemical study of complexes **1–9** and macrocyclic ligands **10–13** was carried out by cyclic voltammetry (CV) and rotating disk electrode (RDE) voltammetry in DMF on a glassy-carbon electrode (GCE), a Pt electrode and, in some cases, an Au electrodes in DMF solutions in the presence of 0.05 M Bu₄NClO₄ as the supporting electrolyte. The electrochemical oxidation and reduction potentials are given in Table 5.

It should be noted that the first oxidation potential (0.78 V relative to Ag|AgCl|KCl(satur.)) and the first reduction potential (-1.64 V) of thiosalen N₂S₂ complex **1**

Table 5. Electrochemical oxidation potentials (E^{Ox}) and reduction potentials (E^{Red}) of the complexes and ligands in DMF (concentration was $3 \cdot 10^{-4}$ mol L $^{-1}$) in the presence of 0.05 M Bu $_4$ NClO $_4$ measured at glassy-carbon (GC) and Pt electrodes relative to Ag|AgCl|KCl(satur.)

Com- pound	E^{Ox}/V		$-E^{\text{Red}}/\text{V}$	
	GC	Pt	GC	Pt
1 ^b	0.78/0.72; 1.23/1.16	0.78/0.72; 1.22/1.14	1.64/1.58; 2.21; 2.41	1.64/1.57; 2.20; 2.40
2	1.04; 1.30	1.00; 1.18	1.34(2e)/-0.01	0.91; 1.24/-0.02
3	1.16	1.16	1.28(2e)/0.04	
4	1.16	1.15	1.39(2e)/0.04	1.26
5 ^c	1.15		1.63; 2.06	
6	Is not oxidized		1.30(2e)/-0.05; 2.19; 2.40; 2.75	1.30(2e)/0.00
7	Is not oxidized		1.51(2e)/0.02; 2.08; 2.39; 2.76	1.60(2e)/-0.15; 2.10
8	Is not oxidized		1.57(2e)/0.03; 2.07; 2.34; 2.76	1.56(2e)/-0.08; 2.08
9	Is not oxidized		1.47(2e)/-0.21; 2.11; 2.39; 2.70	1.42(2e)/-0.32; 2.11
10	1.40	1.35	2.14; 2.44; 2.70	2.06 ^d
11	1.45	1.36	2.20; 2.44; 2.94	2.09
12	1.32	1.42	2.07; 2.31 ^e ; 2.71	2.12
13	1.18; 1.40	1.20	2.10; 2.40 ^e ; 2.79	2.02
21 ^f	1.15	1.16	0.94/0.82(1:1); 1.70; 2.47; 2.73	0.96/0.82(1:1); 1.64
Ni(ClO $_4$) $_2$ · 6H $_2$ O			1.24(2e)/-0.16	1.26(2e)/-0.16

^a The reverse peak potential is given after the slash; 2e is a two-electron process.

^b In MeCN; 0.05 M Bu $_4$ NBF $_4$.

^c Since the compound is very poorly soluble, a saturated solution was used.

^d At an Au electrode; no pronounced peaks are observed at a Pt electrode.

^e The low peak.

^f The compound very slowly dissolves in DMF, and dissolution at 60 °C is completed in approximately 40 min. At room temperature, the concentration of $5 \cdot 10^{-4}$ mol L $^{-1}$ is achieved.

are close to the oxidation potential (~ 0.80 V relative to Ag|AgCl|NaCl (0.1 M)³⁴) and reduction potential (-1.65 V relative to a saturated calomel reference electrode²¹) of the salen N $_2$ O $_2$ complex, *i.e.*, the replacement of the coordinated phenoxide ligands with the thiolate ligands has virtually no effect on these redox potentials. However, electrooxidation of the S $_2$ N $_2$ and S $_2$ O $_2$ complexes occurs by different mechanisms. Earlier, it has been demonstrated³⁴ that in solvents having a weak or moderate coordination ability (for example, in MeCN), Ni(Salen) is electropolymerized to give poly-Ni(Salen) through the formation of *ortho*- and *para*-bonds between the Ph rings of the ligands. In a strong donor solvent DMSO, a six-coordinate solvate complex is formed and the metal atom rather than the ligand is oxidized (Ni^{II} \rightarrow Ni^{III}). We have found that electrooxidation of Ni(Thiosalen) **1** in MeCN (0.1 M Bu $_4$ NClO $_4$) at a Pt electrode did not give electroactive polymeric films, *i.e.*, oxidation of complex **1** in MeCN also occurs at the metal atom, as opposed to the oxygen complex.

Complexes with N $_4$ - and N $_2$ O $_2$ -type salicylidene-iminate and diaminiiminato ligands are reduced to give either the corresponding Ni^I complexes or Ni^{II}(L $^{\cdot -}$), *i.e.*, either the metal atom or the ligand are reduced (see the studies^{1,35} and the data considered below). In spite of this

fact, the reactions of even the latter reduced form with electrophiles or radicals occur at the nickel atom and are accompanied by charge transfer from the ligand to the metal. The complexes under consideration are clearly divided into two types according to the electrochemical behavior in the cathodic region in DMF solutions. Compounds **1** and **21** (Figs 4 and 5) belong to the type 1

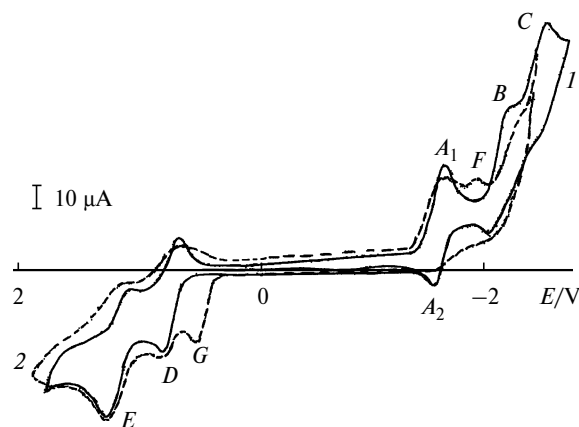


Fig. 4. Cyclic voltammograms of complex **1** (CH $_3$ CN, 0.05 M Bu $_4$ NPF $_6$, the concentration was $5 \cdot 10^{-3}$ mol L $^{-1}$) (**1**) and complex **1** in the presence of an excess ($5 \cdot 10^{-2}$ mol L $^{-1}$) of Bu⁴I (**2**).

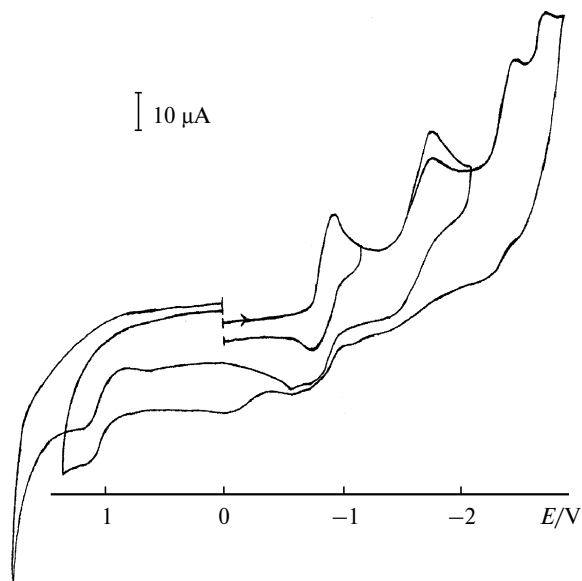
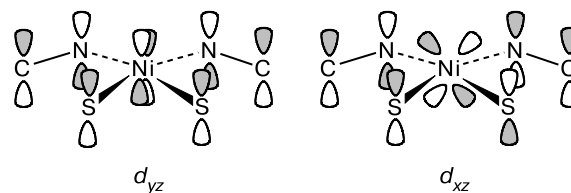


Fig. 5. Cyclic voltammogram of complex **21** (DMF, 0.05 M Bu₄NClO₄, the concentration was 5 · 10⁻⁴ mol L⁻¹ with respect to the monomeric formula).

characterized by reversibility of the first reduction steps. Complexes **2–9** belong to the type 2, which is characterized by irreversible two-electron reduction as the first step accompanied by deposition of Ni metal on the electrode surface (Fig. 6) (this is the reason why the cyclic voltammogram shows a peak of oxidative desorption of nickel with a characteristic triangular shape in the reverse anodic scan).

Structural studies of low-valent Ni complexes (Ni^I and Ni⁰) demonstrated that nickel(0) coordinated by "soft" donor ligands always has a tetrahedral configuration¹ (see also the study³⁵ and references cited therein). The [Ni^I(PMe₃)₄] complex also has a tetrahedral structure. However, reduction of the structurally rigid square-planar Ni^{II} complex with N₄-cyclam to Ni^I leads only to a slight tetrahedral distortion accompanied by elongation of the Ni–N bonds by 0.12 Å.³⁵

A qualitative correlation diagram of the energy levels for the tetrahedral and square-planar nickel complexes, in which binding occurs only through the lone electron pairs of the ligand, is shown in Fig. 7.³⁶ The square-planar complex is characterized by the high-lying unoccupied antibonding b_{1g} orbital (d_{x²-y²} orbital of the metal atom). Upon reduction, this orbital becomes occupied and, hence, the tetrahedral configuration containing additional electrons on the t₂ orbitals becomes more stable. However, the imino groups stabilize low-valence states of the metal due to back donation (interaction between the nonbonding levels of the metal atom (e_g, b_{2g}) and the π* orbital of the C=N group):



These orbitals are lower in energy than the b_{1g} orbitals in the planar complex and than the t₂ orbitals in the pseudotetrahedral complex and are the lowest-energy unoccupied π-type orbitals. This interaction is stronger in the planar configuration than in the tetrahedral one with the result that:

1) the average Ni–ligand bond length in the planar complex is smaller than that in the tetrahedral complex [Ni–N(sp²), 1.68 (D_{4h}) and 1.96 Å (T_d); Ni–S, 2.15 (D_{4h}) and 2.28 Å (T_d)];³⁷

2) the reduction potential of the planar complex should be less negative than those of the pseudotetrahedral complexes, which is actually the case, as can be seen from a comparison of complex **1** with complexes **2–5**.

It is more likely that reduction of the conformationally rigid square-planar complex is accompanied by charge transfer from low-valent nickel to the ligand. The balance between the interactions involving the lone electron pairs of the ligand and the π* orbitals, which stabilize the tetrahedral and planar coordination, respectively, can be such that low-valent nickel in a conformationally rigid system will be more stable than that in flexible complexes, which acquire two electrons, resulting in deposition of nickel metal on the electrode surface.

The electrochemical behavior of complexes **6–9** with macrocyclic ligands is supposedly described by a dissociative mechanism, because Ni^{II} complexes with acyclic tetradentate *S,S'*-dialkylthiosalen-type ligands are unstable²⁵ in DMSO solutions and dissociate to give the diiminodisulfide ligand and Ni²⁺.

The CV curves for reduction of Ni(ClO₄)₂ · 6H₂O and free ligand **13** are shown in Fig. 6, *d*. The reduction of Ni(ClO₄)₂ · 6H₂O was accompanied by the appearance of a two-electron peak in the reverse scan to the anodic region, *viz.*, an anodic peak at +0.16 V. This peak has a characteristic sharp triangular shape and corresponds to oxidative desorption of Ni metal from the electrode surface. The curves shown in Fig. 6, *c* are very similar to the sum of the curves of the free ligand and Ni(ClO₄)₂ (*cf.* Fig. 6, *d*). However, the macrocyclic *S,S'*-polymethylenethiosalen-type ligands do not, apparently, dissociate in DMF solutions to any noticeable degree. This conclusion can be drawn from the following experimental data:

(1) reduction of complexes **6–9** occurs at more negative potentials than the reduction potential of Ni(ClO₄)₂ · 6H₂O;

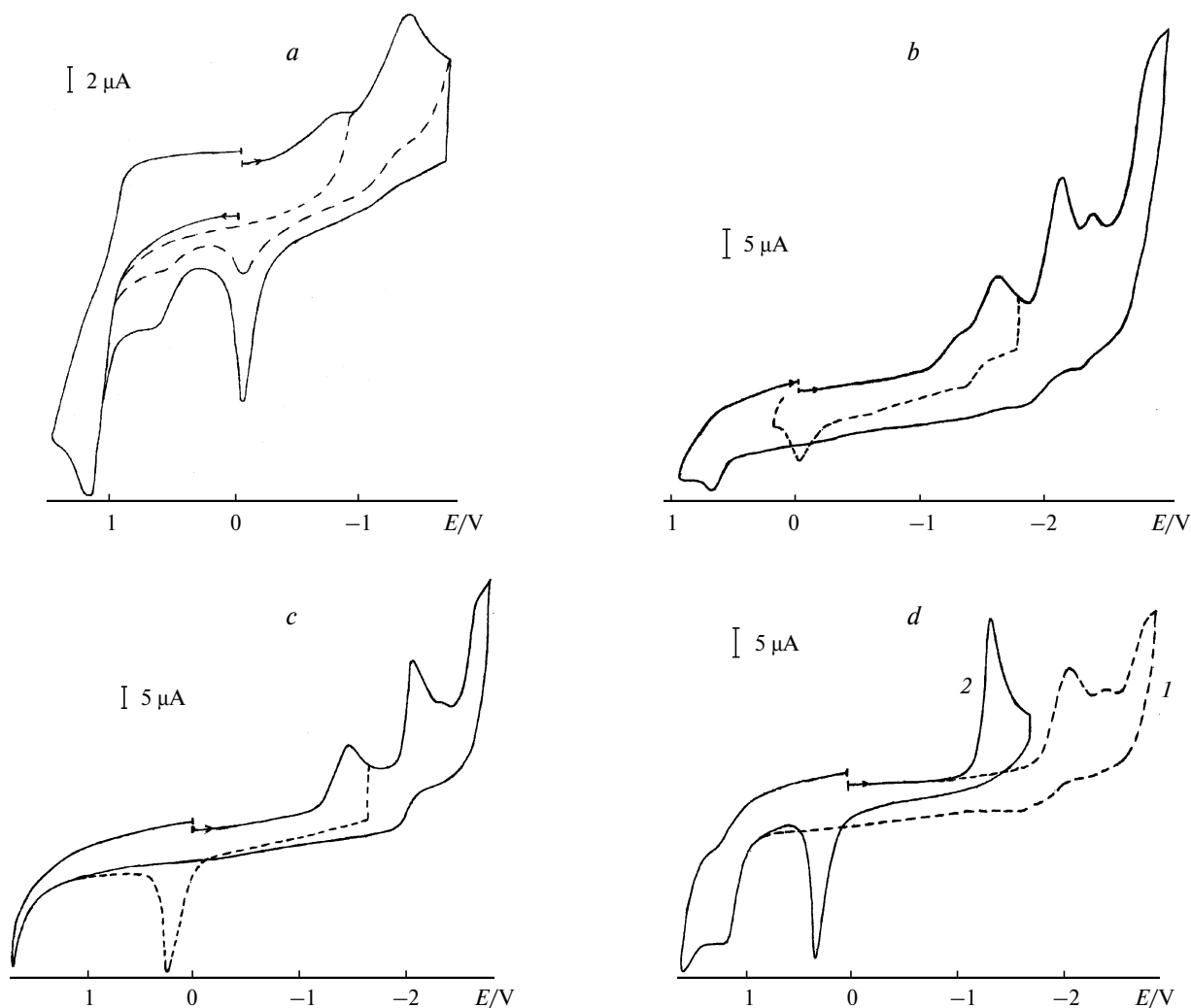


Fig. 6. Cyclic voltammograms (DMF, 0.05 M Bu_4NClO_4) of complexes **3** (a), **8** (b), **9** (c) (CV curves, which were measured after the direction of the potential scan was reversed, are indicated by dashed lines), ligand **13** (d, curve 1), and $\text{NiClO}_4 \cdot 6\text{H}_2\text{O}$ (d, curve 2). The concentrations, mol L^{-1} : $5 \cdot 10^{-4}$ (**3**), $3 \cdot 10^{-4}$ (**8**, **9**), 10^{-3} (**13**, $\text{NiClO}_4 \cdot 6\text{H}_2\text{O}$).

(2) in the region of oxidation of complexes **6–9**, anodic peaks are either absent or strongly shifted to positive potentials compared to the peaks observed for oxidation of the free ligands (see Table 5);

(3) dissolution of the crystals of complexes **6–9** in DMF was not accompanied by the appearance of the green color characteristic of $\text{Ni}(\text{ClO}_4)_2 \cdot 6\text{H}_2\text{O}$ solutions.

Therefore, dissolution of compounds **6–9** in DMF leads, apparently, only to elimination of the coordinated DMSO molecules, resulting in the transformation of compounds **6–9** into square-planar low-spin complexes, due to which their NMR spectra can be measured. Although dissociation of the diiminodisulfide complexes into the starting ligand and Ni^{2+} in DMF cannot be completely ruled out and this process can contribute to the overall

process, the formation of Ni^0 during electrochemical reduction of undissociated complexes plays, apparently, the main role.

It is known that nickel complexes can be divided into two groups according to the electrochemical behavior. The first group includes complexes, which are stepwise reduced through the intermediate formation of Ni^{I} , which is transformed into Ni^0 at substantially higher cathodic potentials. The second group includes complexes, which are electrochemically reduced immediately to the corresponding zero-valent particles in one reversible two-electron step. The first group includes Ni^{II} complexes with cyclams, dmgh, etc., whereas Ni^{II} complexes with the bpy, phen, PPh_3 , or dppe ligands belong to the second group (see the study³⁸ and references cited therein). Reduction affords the 18-electron bis-chelate Ni^0 complex,

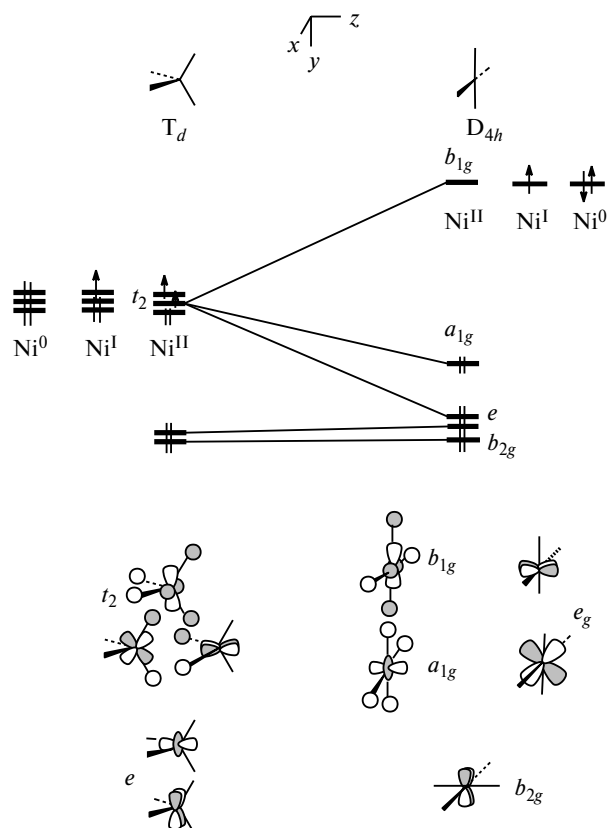
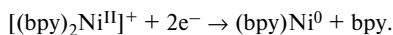


Fig. 7. Correlation diagram of the molecular orbitals of tetrahedral and square-planar complexes containing Ni in different oxidation states (+2, +1, and 0) in the absence of π -bonding.

which loses one chelating ligand to give a 14-electron complex, for example:



For macrocyclic ligands **10–13**, an analogous process cannot occur; instead, Ni metal is eliminated.

For complexes **2–5**, attempts to isolate the corresponding free ligands failed. Hence, these complexes were assigned to the electrochemical type 2 based on the appearance of a peak of oxidative desorption of Ni^0 following the first irreversible two-electron peak in the reverse scan (see Fig. 6, *b*).

We observed an unusual electrochemical situation for the macrocyclic complexes. In the reverse scan to the anodic region, the peak associated with oxidative desorption of nickel metal appeared in the anodic scan after the potential of the first reduction step was achieved. However, the oxidation peak of Ni^0 disappeared, when the reverse scan was carried out at more negative potentials (Fig. 6, *b*, *c*). Therefore, more reduced complexes are more stable and do not eliminate Ni^0 .

In the present investigation, only tentative conclusions about the factors responsible for this phenomenon can be drawn. Let us assume that all electroreduction

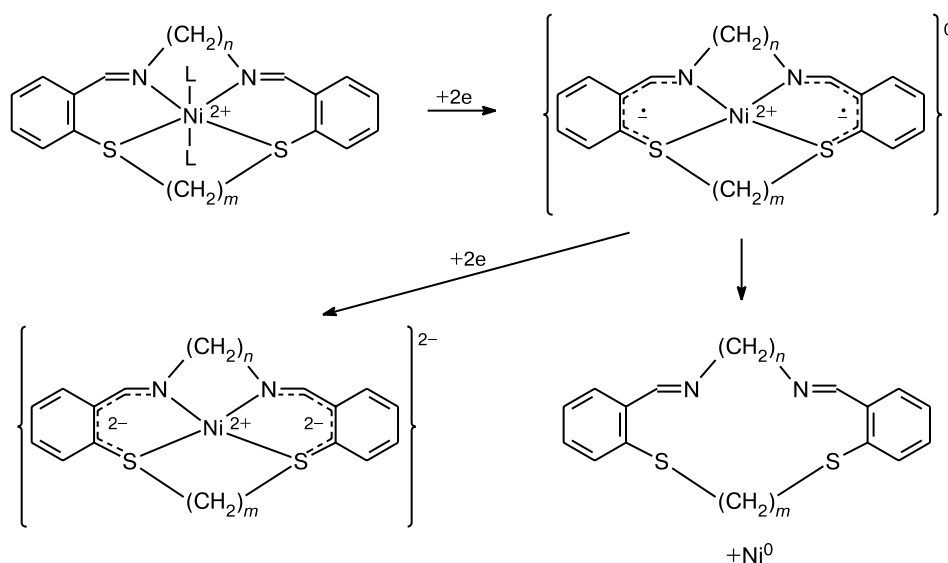
processes occur at the ligand, whereas metal remains in the oxidation state of 2+. Then the initial addition of two electrons gives rise to an electroneutral Ni^{II} complex with the diradical-dianionic ligand in which the charge and spin are delocalized on two independent ($\text{N}=\text{CH}-\text{C}_6\text{H}_4-\text{S}$) $^{\cdot-}$ systems (Scheme 4). Let us then assume that charge transfer from the ligand to metal occurs in the reduced complex giving rise to the corresponding Ni^0 complex with the neutral ligand. This 18-electron complex should have a tetrahedral structure, the transformation to which is substantially hindered by the presence of short bridges between the nitrogen and sulfur atoms. If the coordination unit remains planar or nearly planar, the metal–ligand bonds should be substantially elongated (to decrease destabilization of the antibonding occupied b_{1g} orbital; see Fig. 6), which is also hindered by the bridges. Consequently, two-electron-reduced complexes with the macrocyclic N_2S_2 ligands would be unstable and rapidly undergo decomposition with metal elimination.

At high negative potentials, four-electron reduction of the complexes occurs. Transfer of all electrons to the "ligand" gives rise to the Ni^{II} complex with the tetraanionic ligand (see Scheme 4). In this complex, the acceptor abilities of the π^* orbitals of the C=N groups and the d orbitals of the S atoms are substantially lower and, hence, the $\text{Ni}^0[(\text{L}^{\cdot-}-\text{L}^{\cdot-})^{2-}]$ state (L–L is the macrocyclic ligand) cannot be sufficiently stabilized. However, the square-planar 16-electron $\text{Ni}^{\text{II}}[(\text{L}-\text{L})^{4-}]$ state is stabilized because the initial ligand is transformed to a stronger-field ligand upon reduction. Therefore, instability of the two-electron-reduced complex and stability of the four-electron-reduced complex can be explained assuming that all electrons are initially transferred to the ligand, but the two-electron-reduced complex is more readily transformed into the Ni^0 state (which eliminates nickel) compared to the four-electron reduced complex.

In our laboratory, we used the voltammetric method for the detection of fast alkylation of chelate transition metal complexes based on electrochemical activation of the complexes by one- or two-electron reduction due to which the latter become active in $\text{S}_{\text{N}}2$ reactions with alkylating agents. The criteria for the occurrence of the reaction are as follows: (1) the appearance of a new peak in the cathodic region corresponding to the alkylation product, (2) a strong decrease in reversibility of reduction of the complex, and (3) the appearance of oxidation peaks of I^- , Br^- , or $(\text{dmgH})_2\text{Co}(\text{I})^-$ (for the alkylating agents Bu^nI , Bu^nBr , and $(\text{dmgH})_2\text{CoCH}_3$, respectively). Using complex **1** as an example, we demonstrated that all three agents can be used for alkylation.

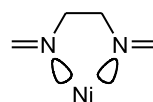
In MeCN (0.05 M Bu_4NPF_6), complex **1** is reduced in three one-electron steps at E_p –1.64, –2.21, and 2.41 V, respectively, and gives two one-electron peaks at E_p 0.76 and 1.26 V in the anodic region (see Fig. 4, curve *I*).

Scheme 4

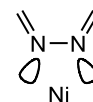


Reversibility of the first reduction peak provides evidence that the Ni^{I} radical anion is stable and can be subjected to alkylation. Upon the addition of, for example, Bu^{PI} (see Fig. 4, curve 2), a new peak (peak F; $E_p = -1.87$ V) is observed already in the first scan. The height of this peak increases with increasing time of electrolysis at the potential of the first peak of compound **1**. In this case, the height of the reverse peak A_1 strongly decreases and the peak corresponding to oxidation of the iodide ion (peak G; $E_p = +0.5$ V) appears in the anodic scan. These changes are indicative of fast electrochemically activated alkylation.³⁸

in thiosalen complex **1**, are directed away from rather than toward the nickel atom:



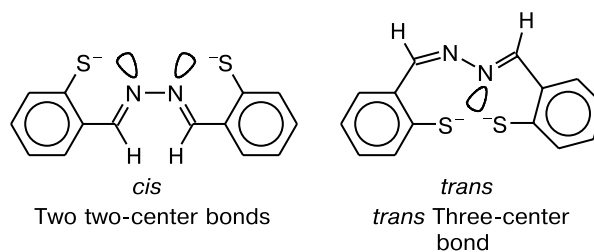
Thiosalen complex

Complex **21**

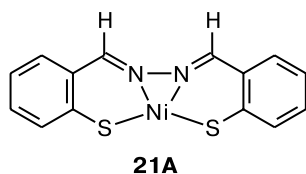
Other possible structures of complex **21**, which are more reasonable from the point of view of the spatial arrangement of the orbitals, can be proposed: two regions of two-center bonding are present in *cis*-**14**, whereas three-center bonding can occur in *trans*-**14**. Then, in addition

Study of the structure of complex **21**

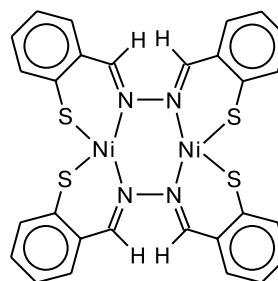
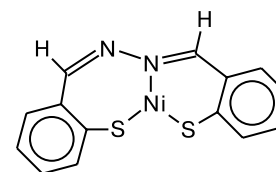
We failed to grow crystals of complex **21** suitable for X-ray diffraction. Below we discuss the possible molecular structures of **21** based on theoretical predictions, spectroscopic characteristics, and electrochemical data. Complex **21** can be *a priori* described by several structural formulas, each corresponding to the simplest molecular formula $\text{Ni}(\text{C}_{16}\text{H}_{12}\text{N}_2\text{S}_2)$.



Two two-center bonds

trans Three-center bond**21A**

Structure **21A** characterized by the cisoid conformation of the $\text{CH}=\text{N}-\text{N}=\text{CH}$ bond system is, apparently, not fully reasonable because the coordinated lone electron pairs of the nitrogen atoms in this structure, unlike those

**21B****21C**

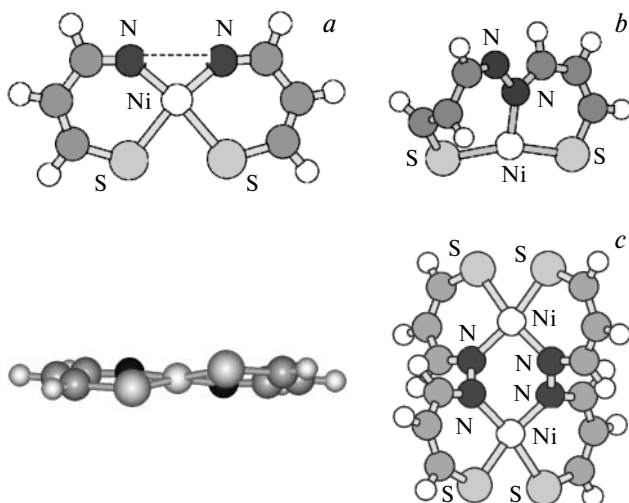
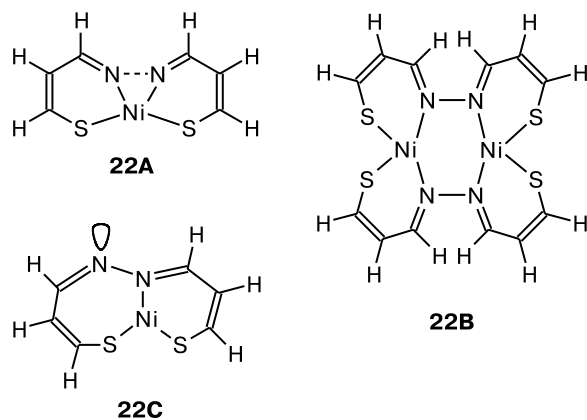


Fig. 8. Structures of model complexes **22A** (a), **22B** (b), and **22C** (c) calculated by the PM3(tm) method.

to the polymeric structure analogous to that shown for complexes **3–5**, the following two structures can be presented: dimeric (**21B**) and monomeric (**21C**) structures containing six- and seven-membered chelate rings, respectively, in which compound **14** serves as either the tetra- or tridentate ligand.

Semiempirical PM3(tm) calculations of model compounds **22A–22C**, which differ from molecules **21–23** in that they have no Ph groups, demonstrated that the N–N bond order in model structure **22A** (Fig. 8, a) analogous to **21A** is as low as 0.3, and the conjugated C=C–C=N bond system in the seven-membered ring in model structure **22C** analogous to **21C** is strongly twisted (dihedral angle is 67°; Fig. 8, b). Only dinuclear structure **22B** analogous to dimer **21B** (Fig. 8, c) has an "adequate" geometry. In calculated structure **22B**, both nickel atoms have an almost planar coordination (improper SNNS dihedral angle is 13°; N–Ni, 1.86 Å; S–Ni, 2.21 Å).



Electrochemical study (see Table 5 and Figs 4 and 5) demonstrated that quasireversible reduction of complex **21**

occurs ~ 0.7 V more easily than that of complex **1**, for which the first reduction step is reversible. Of all the complexes under consideration, complex **21** is most similar in the electrochemical behavior to compound **1**. The UV-Vis spectrum of compound **21** (see Fig. 3) is analogous to the spectrum of thiosalen complex **1** and differs from the spectra of all other compounds under consideration (in addition, complexes **1** and **21** in the solid state and in solution are similar in color). The ESR spectrum of a solution of complex **21** in DMF has no signals, and no noticeable broadening of the lines is observed in the ^1H NMR spectrum. These facts confirm the presence of low-spin diamagnetic Ni^{II} in molecule **21**. The above-mentioned calculated, electrochemical, and spectroscopic data provide evidence that the structure of compound **21** is most likely described by a dimeric structure (**21B**), in which both nickel atoms are in a square-planar coordination environment. It should be emphasized that an unambiguous conclusion about the structure of compound **21** can be drawn only based on the results of additional investigation.

However, it should be noted that the mass spectrum of compound **21** (direct probe, electron impact, 70 eV) has no peaks corresponding to molecular ions of the dimer or monomer (m/z 656 or 328), and the largest mass of the fragment ion is 299.

Experimental

Materials, electrodes, apparatus, and methods. Dithiosalicylaldehyde was synthesized according to a known procedure.³⁹ Thiosalicylaldehyde was prepared according to a procedure published earlier.⁴⁰ *S-tert*-Butylthiosalicylaldehyde was synthesized from *ortho*-nitrobenzaldehyde and *tert*-butanethiol according to a known procedure.³¹ Complexes **1**²⁸ and **2**²⁹ were prepared as described earlier.

Dimethylformamide of high-purity grade was purified by successive refluxing and vacuum distillation over anhydrous CuSO_4 and P_2O_5 .

The ^1H NMR spectra were recorded on a Varian-VXR-400 instrument at 400 MHz.

The IR spectra were measured on a UR-20 instrument in a thin film or Nujol mulls.

The UV-Vis spectra were recorded on Specord-M40 (200–900 nm) and Helios- α Nicolet (200–1100 nm) instruments in a 0.1-cm quartz cell at 20–22 °C.

The mass spectra were measured on a Varian MAT 202 instrument (direct probe, electron impact, 70 eV).

Study of compound **21** by ESR spectroscopy in a DMF solution (concentration was $\sim 5 \cdot 10^{-4}$ mol L^{-1}) was carried out on a Bruker EMX 6-1 radiospectrometer at room temperature and at 77 K.

X-ray diffraction study of compound **8** was performed on an Enraf Nonius CAD-4 diffractometer (graphite monochromator, $\lambda(\text{MoK}\alpha) = 0.71069$) equipped with a scintillation detector at room temperature. The structure was solved by direct methods (CSD program⁴¹) and refined by the full-matrix least-squares

method against F with anisotropic displacement parameters for all nonhydrogen atoms using the JANA2000 program package.⁴² The positions of the hydrogen atoms were not revealed.

Electrochemical studies were carried out on a PI-50-1.1 potentiostat. Glassy-carbon ($\phi = 1.8$ mm) or platinum ($\phi = 3.5$ mm) disks were used as the working electrodes; a 0.05 M Bu_4NClO_4 solution in DMF or a 0.05 M Bu_4NPF_6 solution in MeCN served as the supporting electrolyte; Ag/AgCl/KCl(satur.) was used as the reference electrode. All measurements were carried out on stationary or rotating electrodes at a potential scan rate varying from 20 to 500 mV s^{-1} under argon.

Quantum-chemical calculations were carried out using the semiempirical SCF PM3 method,³³ which was extended by including the parameters for all first-row transition metals and selected second- and third-row transition metals. This extended method (PM3(tm)) is implemented in the HyperChem program package (HyperCube Inc., FL, USA). Geometry optimization of the molecules was carried out with a gradient of no higher than 10 $\text{kal} (\text{\AA mol})^{-1}$ as the convergence criterion.

The spectroscopic data and results of elemental analysis for the free ligands and intermediates of their synthesis are given in Table 1. The corresponding data for the nickel complexes are listed in Table 2. The yields of the products are given in the schemes presented in the text.

Synthesis of ligands

Macrocyclic *S*-alkylthiosalicylimines 10–13 (general procedure). α,ω -Bis(2-formylphenyl)- α,ω -dithiaalkane **13** or **14** (4 mmol) was suspended in methanol or ethanol (20 mL). Then diamine (1,2-diaminoethane or 1,3-diaminopropane) (4 mmol) was added and the reaction mixture was stirred at room temperature for 30 min until α,ω -bis(2-formylphenyl)- α,ω -dithiaalkane was completely dissolved. Then anhydrous MgSO_4 (2 g) was added to the solution and the reaction mixture was stirred for 4 h and filtered off. The drying agent was washed with EtOH and the combined solutions were concentrated *in vacuo* to obtain a yellow oil with a small amount of white crystals. The mixture was dissolved in chloroform (5 mL), the crystals that remained undissolved were filtered off, and the solution was concentrated. The target diimine as a yellow oil was used in the synthesis of the complexes.

***N,N'*-Polymethylenebis(*ortho-tert*-butylthiobenzal)diimines 15–17 (general procedure).** *ortho-tert*-Butylthiobenzaldehyde (0.77 g, 4 mmol) was dissolved in benzene (60 mL) and the corresponding diamine (2 mmol) was added. The reaction mixture was refluxed using a Dean–Stark trap for 3 h. The residual benzene was removed *in vacuo*. The yellow oil, which crystallized with time, was used in the synthesis of the complexes without additional purification. The complexes were prepared in ~100% yields.

1,4-Bis(2-formylphenyl)-1,4-dithiabutane (18). *ortho*-Nitrobenzaldehyde (3 g, 0.02 mol) and ethane-1,2-dithiol (1 g, 0.011 mol) were dissolved in DMF (25 mL) and then finely dispersed potassium carbonate (3 g, 0.02 mol) was added. The reaction mixture was stirred at 60 °C for one day, filtered, and concentrated to 5 mL, after which ethanol (20 mL) was added. A yellow flocculent precipitate that formed upon cooling (m.p. 119 °C) was filtered off and dissolved in a minimum amount of DMF. The product was precipitated with a 1 : 1 mixture of

ethanol and diethyl ether to prepare compound **13** as a white powder in a yield of 1.15 g (38%), m.p. 131 °C (lit. data⁴³: 133 °C).

1,5-Bis(2-formylphenyl)-1,5-dithiapentane (19). *ortho*-Nitrobenzaldehyde (3 g, 0.02 mol) and propane-1,3-dithiol (1.2 g, 0.011 mol) were dissolved in DMF (25 mL) and then finely dispersed potassium carbonate (3 g) was added. The reaction mixture was stirred at 60 °C for two days, filtered, and concentrated to 5 mL. Then ethanol (20 mL) was added. Cooling of the mixture afforded a white precipitate, which was filtered off and recrystallized from ethanol to prepare compound **19** as a white powder in a yield of 1.77 g (56%), m.p. 51–53 °C (lit. data⁴³: 54–56 °C).

Di(*ortho-tert*-butylthiobenzal)azine (20). *ortho-tert*-Butylthiobenzaldehyde (0.77 g, 4 mmol) and hydrazine hydrate (0.03 g, 2 mmol) in benzene (60 mL) were stirred at room temperature for 0.5 h. Then the mixture was slowly brought to boiling and refluxed for 3 h using a Dean–Stark trap. The solvent was removed *in vacuo* and the oily product was used without additional purification.

Synthesis of complexes

Complexes of *N,N'*-polymethylenebis(*ortho*-thiobenzal)diimines and di(*ortho-tert*-butylthiobenzal)azine with Ni^{II} (general procedure). The corresponding *N,N'*-polymethylenebis(*ortho*-thiobenzal)diimine **15–17** or di(*ortho-tert*-butylthiobenzal)azine **20** (1 mmol) in anhydrous ethanol (3 mL) was mixed with anhydrous nickel chloride (0.13 g, 1 mmol). The reaction mixture was refluxed for 4 h and cooled to ~20 °C. The finely dispersed pale-green precipitate was filtered off, washed successively with anhydrous ethanol and anhydrous diethyl ether, and dried in air. All complexes are poorly soluble in DMF and insoluble in other organic solvents and water.

***S*-Alkylthiosalicylimine complexes of Ni^{II} (general procedure).** Macrocyclic diiminobis(sulfides) **10–13** were dissolved in a minimum volume of chloroform, 1–2 drops of DMSO were added, and the reaction mixture was mixed with an equimolar amount of $\text{Ni}(\text{ClO}_4)_2 \cdot 6\text{H}_2\text{O}$ dissolved in a minimum volume of ethanol. The reaction mixture was refluxed for 20 min. After cooling to 0 °C, the crystals that precipitated were filtered off, washed with a small amount of ethanol, and dried in air.

References

1. M. Calligaris and L. Randaccio, in *Comprehensive Coordination Chemistry*, Eds G. Wilkinson, and R. D. Gillard, Pergamon, Oxford, 1987, **2**, Ch. 20.
2. A. K. Jorgensen, *Chem. Rev.*, 1989, **89**, 431.
3. P. J. Pospisil, D. H. Carsten, and E. N. Jacobsen, *Chem. Eur. J.*, 1996, **2**, 744 (and references cited therein).
4. K. P. Bryliakov and E. P. Talsi, *Inorg. Chem.*, 2003, **42**, 7258.
5. T. Fukuda and L. Katsuki, *Tetrahedron*, 1997, **53**, 7201.
6. J. Du Bois, C. S. Tomooka, J. Hong, and E. M. Carreira, *Acc. Chem. Res.*, 1997, **30**, 364.
7. C. Bolm and F. Bienewald, *Angew. Chem., Int. Ed. Engl.*, 1995, **34**, 2640.
8. T. Fukuda and L. Katsuki, *Tetrahedron Lett.*, 1997, **38**, 3435.
9. S. E. Schaus, J. Branalt, and E. N. Jacobsen, *J. Org. Chem.*, 1998, **63**, 403.

10. M. D. Kaufman, P. A. Greico, and D. W. Bougie, *J. Am. Chem. Soc.*, 1993, **115**, 11648.
11. J. F. Larrow and E. N. Jacobsen, *J. Am. Chem. Soc.*, 1994, **116**, 12129.
12. K. Hamachi, R. Irie, and L. Katsuki, *Tetrahedron Lett.*, 1996, **37**, 4979.
13. E. N. Jacobsen, F. Kakiuchi, R. G. Konsler, J. F. Larrow, and M. Tokunaga, *Tetrahedron Lett.*, 1997, **38**, 773.
14. M. Tokunaga, J. F. Larrow, F. Kakiuchi, and E. N. Jacobsen, *Science*, 1997, **277**, 936.
15. J. L. Leighton and E. N. Jacobsen, *J. Org. Chem.*, 1996, **61**, 389.
16. L. E. Martinez, J. L. Leighton, D. H. Carsten, and E. N. Jacobsen, *J. Am. Chem. Soc.*, 1995, **117**, 5897.
17. R. L. Puddock and S. T. Nguyen, *J. Am. Chem. Soc.*, 2001, **123**, 11498.
18. J. M. Ready and E. N. Jacobsen, *J. Am. Chem. Soc.*, 2001, **123**, 403.
19. A. A. Isse, A. Gennaro, and E. Vianello, *J. Electroanal. Chem.*, 1998, **444**, 241.
20. V. G. Koshechko and V. D. Pokhodenko, *Izv. Akad. Nauk, Ser. Khim.*, 2001, 1843 [*Russ. Chem. Bull., Int. Ed.*, 2001, **50**, 1929].
21. A. A. Stepanov, M. G. Peterleitner, S. M. Peregudova, and L. I. Denisovich, *Elektrokhimiya*, 2002, **38**, 630 [*Russ. J. Electrochem.*, 2002, **38** (Engl. Transl.)].
22. D. P. Riley, *Chem. Rev.*, 1999, **99**, 2573.
23. V. K. Sivasubramanian, M. Ganesan, S. Rajagopal, and R. Ramaraj, *J. Org. Chem.*, 2002, **67**, 1506.
24. A. Cristensen, H. S. Jensen, V. McKee, C. J. McKenzie, and M. Munch, *Inorg. Chem.*, 1997, **36**, 6080.
25. D. S. Bohle, A. Zafar, P. A. Goodson, and D. A. Jaeger, *Inorg. Chem.*, 2000, **39**, 712.
26. M. H. Chisholm, E. R. Davidson, J. C. Huffman, and K. B. Quinian, *J. Am. Chem. Soc.*, 2001, **123**, 9652.
27. S. V. Kryatov, B. S. Mohanraj, V. V. Tarasov, O. P. Kryatova, and E. V. Rybak-Akimova, *Inorg. Chem.*, 2002, **41**, 923.
28. N. Goswami and D. Eichhorn, *Inorg. Chem.*, 1999, **38**, 4329.
29. M. F. Corrigan and B. O. West, *Aust. J. Chem.*, 1976, **29**, 1413.
30. B. Xie, L. Wilson, and D. Stanbury, *Inorg. Chem.*, 2001, **40**, 3606.
31. T. Yamamura and M. Tadokoro, *Chem. Lett.*, 1989, **7**, 1245.
32. F. H. Allen and O. Kennard, *Chem. Des. Autom. News*, 1993, **8**, 1.
33. J. J. P. Stewart, *J. Comput. Chem.*, 1989, **10**, 209.
34. M. Vilas-Boas, C. Freire, B. de Castro, P. A. Christensen, and A. R. Hillman, *Inorg. Chem.*, 1997, **36**, 4919.
35. G. Music, J. H. Riebenspies, and M. Y. Darensbourg, *Inorg. Chem.*, 1998, **37**, 302.
36. K. P. Butin, R. D. Rakhimov, and I. G. Il'ina, *Izv. Akad. Nauk, Ser. Khim.*, 1999, 71 [*Russ. Chem. Bull., Int. Ed.*, 1999, **49**, 71].
37. K. W. Muir, *Molecular Structure by Diffraction Methods*, Vol. 1, Chemical Society, London, 1973, p. 580.
38. E. K. Beloglazkina, A. A. Moiseeva, A. V. Churakov, I. S. Orlov, N. V. Zyk, J. A. K. Howard, and K. P. Butin, *Izv. Akad. Nauk, Ser. Khim.*, 2002, 436 [*Russ. Chem. Bull., Int. Ed.*, 2002, **51**, 467].
39. H. S. Kasmai and S. G. Tadokoro, *Synthesis*, 1989, 763.
40. D. Leaver, J. Smolicz, and W. H. Stafford, *J. Chem. Soc.*, 1962, 740.
41. L. G. Akselrud, Yu. N. Gryn, P. V. Zavalij, V. K. Pecharsky, and V. S. Fundamensky, *Abstrs of the 12th European Crystallographic Meeting*, Moscow, 1989, p. 155.
41. V. Petricek and M. Dusek, *Jana2000. The Crystallographic Computing System*, Institute of Physics, Praha, Czech Republic, 2000.
42. L. Lindoy and R. Smith, *Inorg. Chem.*, 1981, **20**, 1314.

*Received March 5, 2004;
in revised form November 1, 2004*